Electronic Supplementary Information

Relating the composition and interface interactions in the hard corona of gold nanoparticles to the induced response mechanisms in living cells

Gergo Peter Szekeres[1,2], Stephan Werner[3], Peter Guttmann[3], Cecilia Spedalieri[2], Daniela Drescher[2], Vesna Živanović[1,2], Maria Montes-Bayón[1,4], Jörg Bettmer[4], Janina Kneipp[1,2,*]

1 Humboldt-Universität zu Berlin, School of Analytical Sciences Adlershof, Albert-Einstein-Str. 5-9, 12489 Berlin, Germany

2 Humboldt-Universität zu Berlin, Department of Chemistry, Humboldt-Universität zu Berlin, Brook-Taylor-Str. 2, 12489 Berlin, Germany

3 Helmholtz-Zentrum Berlin für Materialien und Energie GmbH, Department X-ray Microscopy, Albert-Einstein-Str. 15, 12489 Berlin, Germany

4 University of Oviedo, Department of Physical and Analytical Chemistry, Faculty of Chemistry and Instituto de Investigación Sanitaria del Principado de Asturias (ISPA), C/ Julian Clavería 8, 33006 Oviedo, Spain

Table of contents:

* For Table S1 and Table S2, containing detailed proteomics information, please refer to the additional separate files.

Characterization of the gold nanoparticles and their aggregates

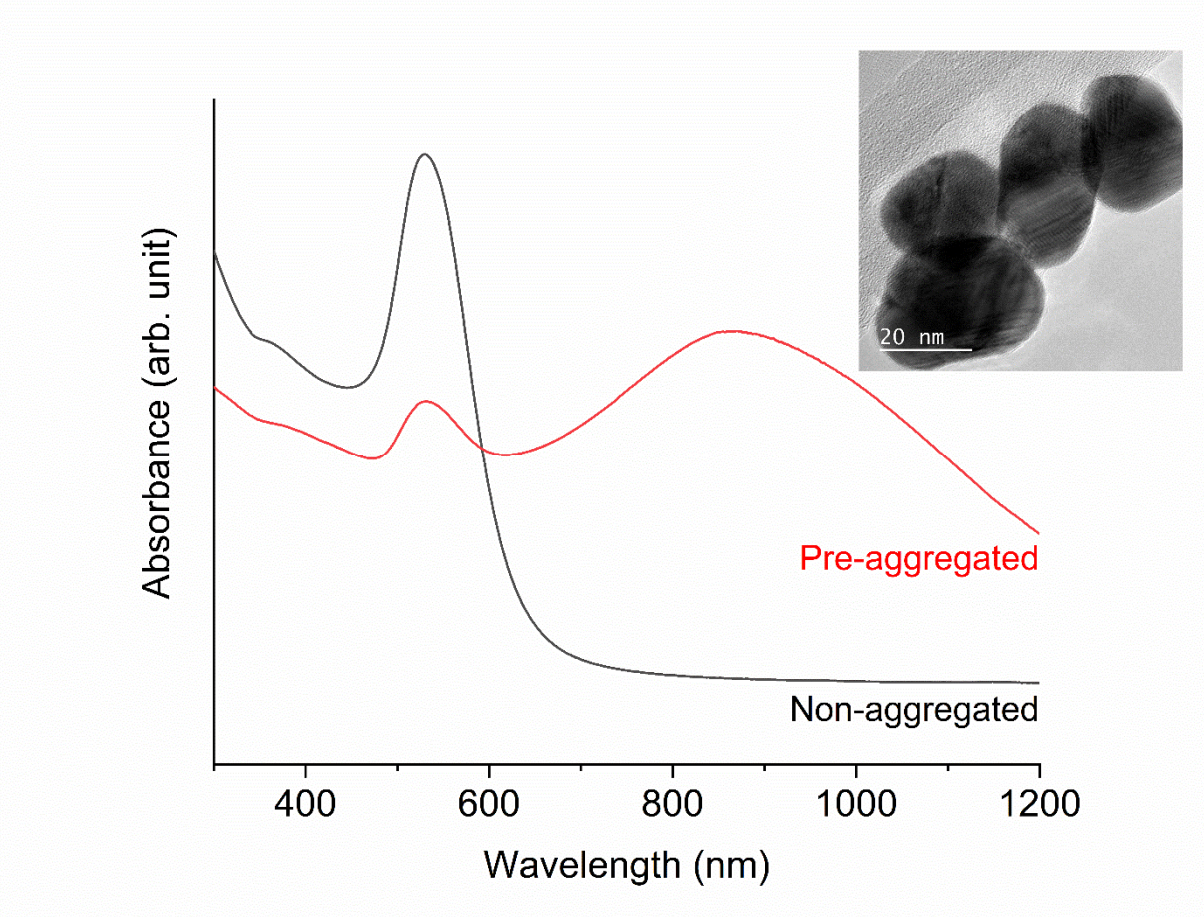

Figure S1. UV-vis spectra of the non-aggregated gold nanoparticles (black trace) and the pre-aggregated gold nanoparticles (red trace). Inset: transmission electron micrograph of the gold nanoparticles.

Supporting data from cryo-SXT

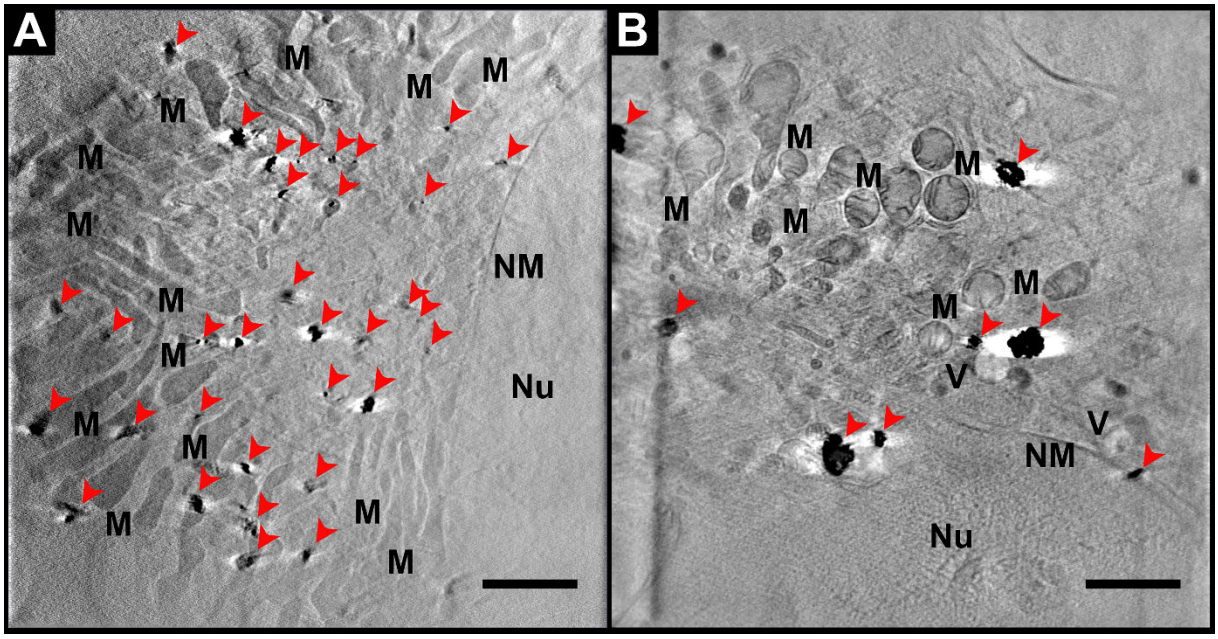

Figure S2. Tomographic slices of A549 cells incubated with (A) non-aggregated and (B) pre-aggregated gold nanoparticles, respectively, in DMEM-FBS. Scale bar: 2 µm. Intracellular gold nanostructures are marked with red arrowheads. M: mitochondrion, V: vesicle, Nu: nucleus, NM: nuclear membrane.

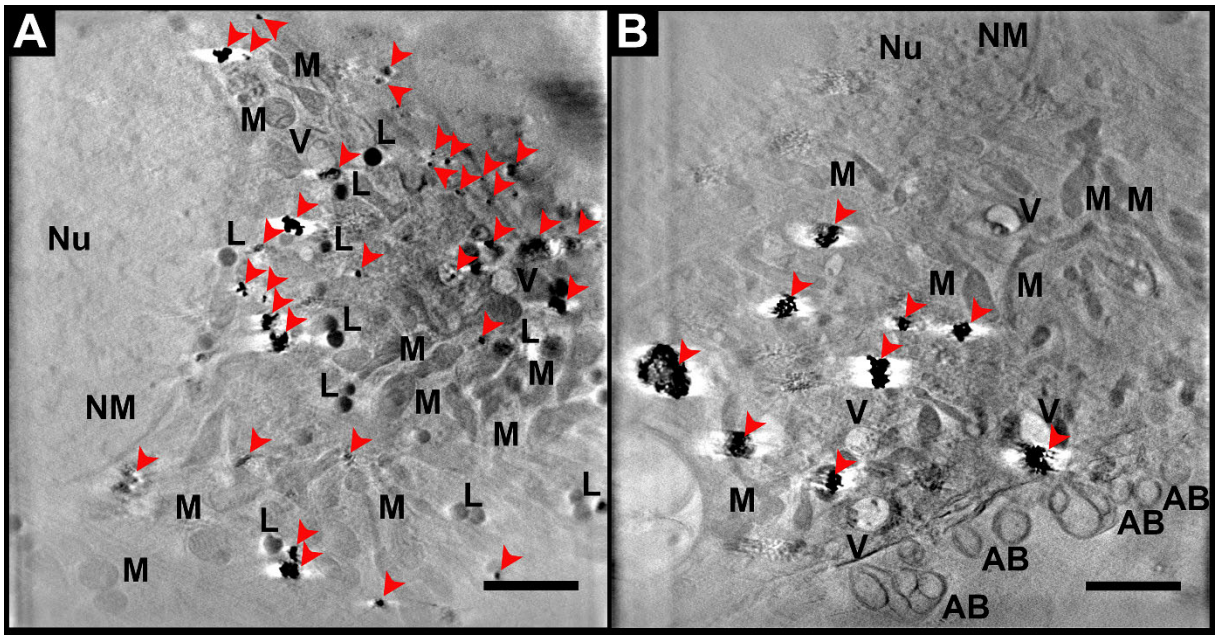

Figure S3. Tomographic slices of A549 cells incubated with (A) non-aggregated and (B) pre-aggregated gold nanoparticles, respectively, in McCoy-FBS. Scale bar: 2 µm. Intracellular gold nanostructures are marked with red arrowheads. M: mitochondrion, L: lipid droplet, V: vesicle, Nu: nucleus, NM: nuclear membrane, AB: apoptotic body.

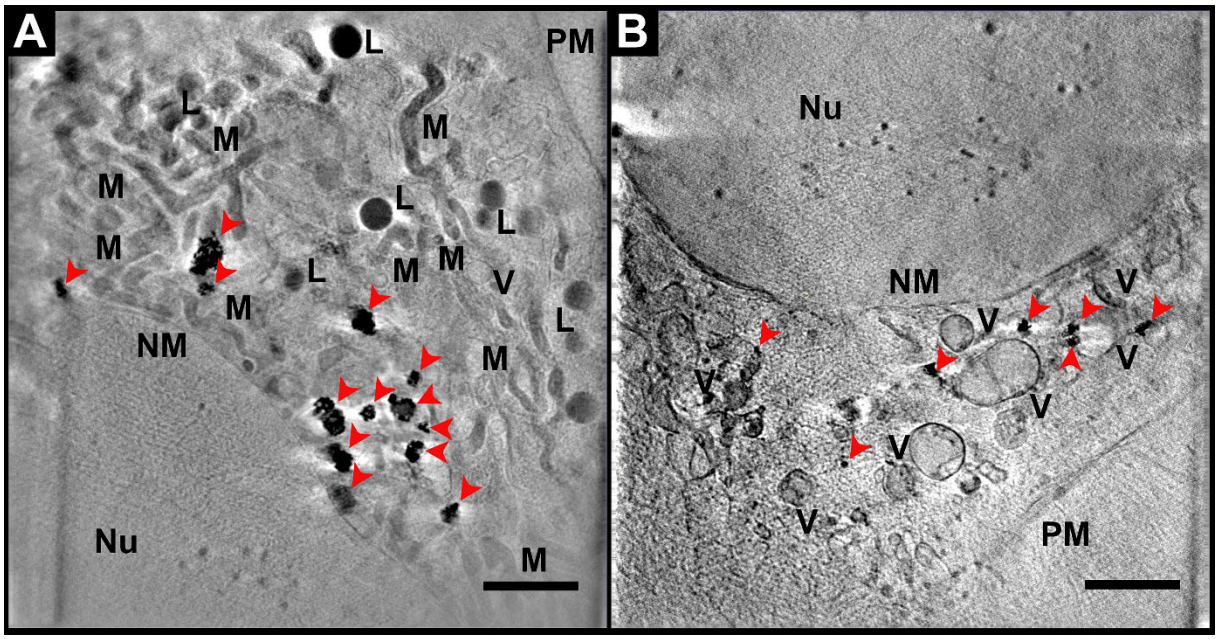

Figure S4. Representative tomographic slices of HCT-116 cells incubated with pre-aggregated gold nanoparticles in (A) DMEM-FBS and in (B) McCoy-FBS, respectively. Scale bar: 2 µm. Intracellular gold nanostructures are marked with red arrowheads. M: mitochondrion, L: lipid droplet, V: vesicle, Nu: nucleus, NM: nuclear membrane, PM: plasma membrane.

XTT viability test

The changes in cell viability as a result of their incubation with gold nanoparticles were studied with an XTT cell proliferation assay kit. The following samples were prepared for the cell viability studies: (i) cells without nanoparticles (positive control); (ii) cells incubated with the 1:10 mixture of non-aggregated gold nanoparticles and the respective culture medium; (iii) cells incubated with the 1:10 mixture of pre-aggregated gold nanoparticles and the respective culture medium; (iv) cells incubated with Triton X-100 (negative control); and (v) cells incubated with the 1:10 mixture of non-aggregated gold nanoparticles and the respective culture medium, then with Triton X-100 (negative control).

Sample preparation

XTT tests were performed with a commercial XTT cell proliferation assay (Cayman Chemical, Michigan, USA). The samples were analyzed with a Multimode Plate Reader, Victor X5 (Perkin-Elmer, Berlin, Germany) operating in absorbance mode. A549 and HCT-116 cells were cultured in clear, flat bottom Greiner-type 96-well plates. Based on experience, HCT-116 cells grew slower in DMEM-FBS than in McCoy-FBS; therefore ~5000 cells and ~2,500 cells were pipetted into each well in the experiments with DMEM-FBS and McCoy-FBS, respectively. A549 cells showed comparable growth in both media, and ~2,000 cells were transferred into each well in the XTT experiments.

At least four sample replicates were studied for each incubation condition. Pure gold nanoparticles, pure culture media, and the 1:10 mixture of the nanoparticles and the culture media were analyzed as control samples. Each control was analyzed with and without the XTT assay to determine whether the background signal from the pristine samples contributes significantly to the absolute absorbance.

The incubation with gold nanoparticles was started at least 24 h after seeding the cells into the 96-well plate. Every sample was prepared in two series: one with and one without XTT assay to make sure the absorbance of the pure sample was negligible in the analysis.

Results

Cells grown in different culture media show opposite tendencies: while a decreasing tendency was found in the viability of both cell lines in McCoy-FBS, it was reversed in DMEM-FBS. The results are summarized in Figure S4. The viabilities observed in XTT in McCoy-FBS are in agreement with the viability inferred based on the cryo-SXT results (compare Figure 2 in the main text, S1, and S3 with the red bars in S4). In HCT-116 (compare Figure 2B in the main text with the red bars in Figure S4A), the administration of non-aggregated gold nanoparticles lowered the viability to 91%, while the strong cellular stress induced by the uptake of pre-aggregated gold nanoparticles resulted in a relative viability of 64% (compare Figure S3B with the red bars in Figure S4A). In contrast, the viability of A549 cells did not change after incubation with non-aggregated gold nanoparticles, and it only decreased to 85% after the administration of pre-aggregated gold nanoparticles.

These results indicate that HCT-116 cells are more sensitive to the presence of internalized gold nanoparticles than A549 cells. The sensitivity of HCT-116 to gold nanoparticles could be explained by the lack of vimentin in the hard corona due to the different processing of the nanoparticles as opposed to A549 as discussed in the manuscript text (Tables S1 and S2), as vimentin reduces oxidative stress, the primary reason of mitochondrial and ribosomal

damage.[1] Therefore, the high abundance of proteins originating from mitochondria and ribosomes in the hard corona formed in HCT 116 (Table S1) can be explained by the lack of vimentin, and thus the more prominent generation of reactive oxygen species and the resulting oxidative stress,[1] as discussed in the main text.

Based on the cryo-SXT experiments and light microscopic observations of the cultures, it is evident that the cell viability cannot increase to values over 100% (Figure S4 green bars). The XTT dye is transformed into its measured form in the mitochondria,[2] thus, the higher viability values with increasing nanoparticle uptake are possibly the result of a higher number of functioning mitochondria in DMEM-FBS (see Figure 2A in the main text) due to the induced cellular stress upon nanoparticle internalization. When A549 cells were incubated with non-aggregated gold nanoparticles (Figure S4B green bars), only a mild increase in the number of mitochondria was observed in DMEM-FBS compared to the sample incubated in McCoy-FBS (Figures S1A and S2A). This small increase is reflected in the viability results in the two media, rendering the nominal viability of A549 cells slightly higher in DMEM FBS. The difference is larger in the case of incubation with pre-aggregated gold nanoparticles, as the viability in McCoy-FBS drops while that in DMEM-FBS increases (Figure S4B). This difference can be attributed to the mitochondrial fission observed in Figure S1B. In the case of HCT-116 (Figure 2 in the main text and Figure S3, and the green bars in Figure S4A), the increasing tendency in the nominal viability in DMEM-FBS is less steep than in A549, which is probably due to the more prominent drop in the number of viable cells.

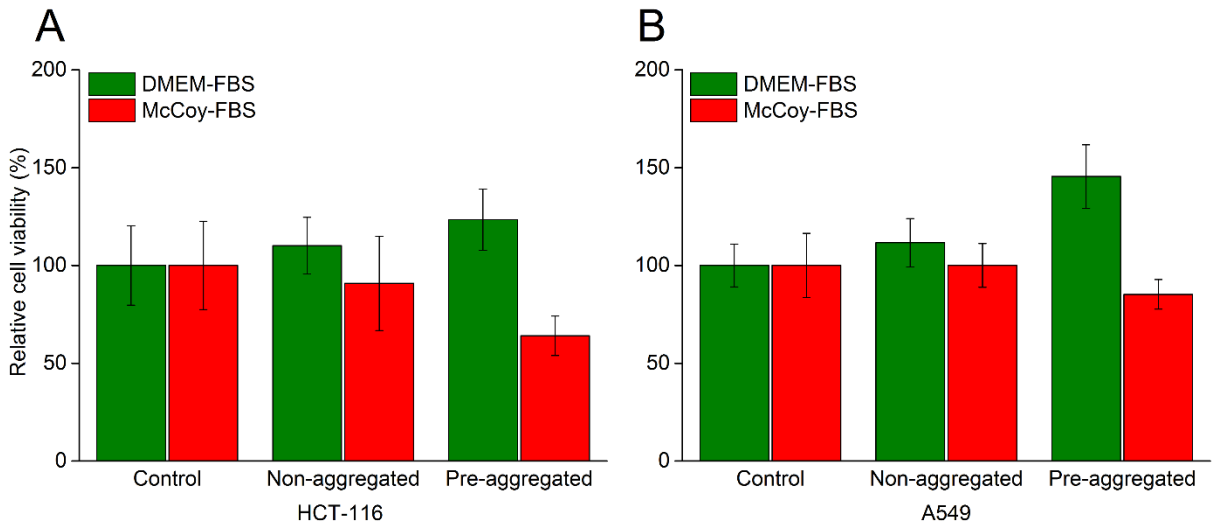

Figure S5. Relative cell viability values calculated from XTT results of (A) HCT-116 cells and (B) A549 cells under different incubation conditions. The error bars represent the distribution of the measured cell viability based on t-test.

Average SERS spectra

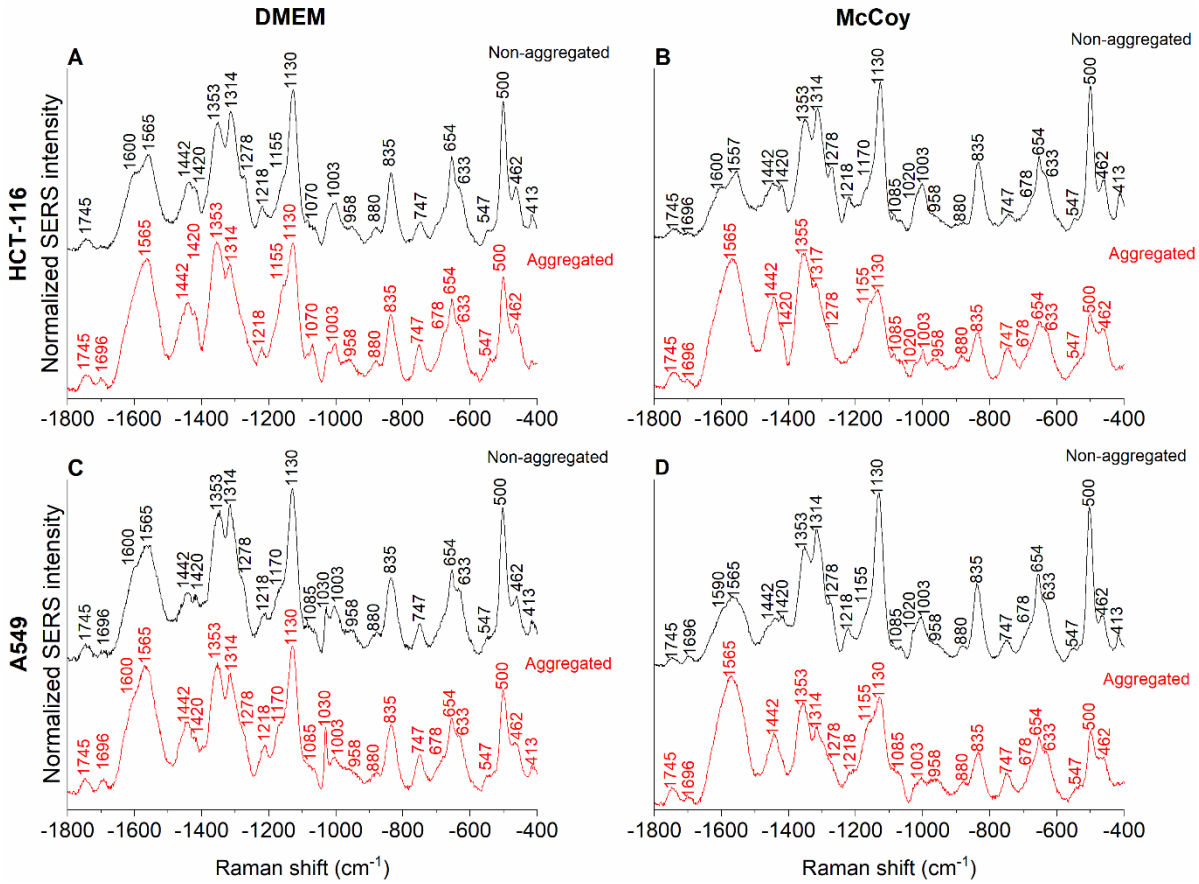

Figure S6. SERS spectra of HCT-116 cells grown in (A) DMEM-FBS and (B) McCoy-FBS, and of (C) A549 cells grown in DMEM-FBS and (D) McCoy-FBS (D). 24 h incubation, excitation wavelength: 785 nm, acquisition time: 1 s, excitation intensity: 2.3×10^5 W/cm^2. Each spectrum is an average of all individual spectra collected from five cells, corresponding to 400-900 spectra depending on the respective data set (for details cf. caption of Figure 5).

Analysis of the rendered intracellular nanoparticle aggregates

Table S3. Number of nanoparticles per tomogram after incubation with gold nanoparticles and nanoaggregates for 24 hours, estimated from the number and size of nanoparticles obtained by segmentation of tomograms of selected individual cells.

	Incubated with non-aggregated nanoparticles			**Incubated with pre-aggregated nanoparticles**		
Cell line Medium	**Nanoparticles per Aggregates**	**Nanoparticles per Cell**	**Number of Aggregates**	**Nanoparticles per Aggregates**	**Nanoparticles per Cell**	**Number of Aggregates**
HCT-116 DMEM	109	10459	96	108	20234	187
HCT-116 McCoy	138	8391	61	113	9071	80
A549 DMEM	66	15005	228	242	33652	139
A549 McCoy	112	15193	136	212	24551	116

Tentative band assignments

Table S4. Raman shifts and their tentative assignments in the spectra displayed in Figure 5 and Figure S5. Abbreviations: *v* stretching, *δ* deformation, *symm* symmetric, *wag* wagging, *br* breathing, *R* benzene ring, *r* pyrrole ring. Band assignments were based on refs. [3-9].

Raman shift (cm^{-1})	Tentative assignment
1745	ν(C=O)
1696	Amide I
1600	Tyr, Phe ν(R), Amide I
1590	ν(C=C), COO^-
1565	Amide II, Trp, Tyr, ν(COO^-)
1557	Amide II, Trp, Tyr, ν(COO^-)
1442	δ(CH_2)
1420	A, G, CH_3CH_2 twisting
1353	Trp, G
1314	G, δ(C-H), Amide III
1278	Amide III, CH_2 wag, DNA/RNA
1218	Amide III, T, A, ν(PO_2,C-N)
1170	C, G, Tyr C-H bend, lipids
1155	ν(C-C, C-N)
1130	ν(C-C, C-N)
1085	ν(C-C, C-N)
1070	ν(C-C), ν(PO_2) of DNA/RNA, Pro
1030	Phe, ν(C-C)
1020	ν(C-O) of ribose
1003	R br
958	ν(C-C) of Pro and Val
880	ν(C-C) of Pro and Val
835	$\nu(O\text{-}P\text{-}O)_{asymm}$, Tyr, Pro
747	T, ν(C-S,C-C), Pro, Trp symm br
678	ν(C-S), G, T
654	ν(C-S), C-C twisting of Tyr, Phe
633	ν(C-S), C-C twisting of Tyr, Phe
547	ν(S-S), cholesterol
500	ν(S-S)
462	ν(C-S)
413	Trp

References

1. Haversen, L.; Sundelin, J. P.; Mardinoglu, A.; Rutberg, M.; Stahlman, M.; Wilhelmsson, U.; Hulten, L. M.; Pekny, M.; Fogelstrand, P.; Bentzon, J. F.; Levin, M.; Boren, J., Vimentin deficiency in macrophages induces increased oxidative stress and vascular inflammation but attenuates atherosclerosis in mice. *Sci. Rep.* **2018,** *8* (1), 16973.

2. Altman, F. P., Tetrazolium Salts and Formazans. *Prog. Histochem. Cyto.* **1976,** *9* (3), III-51.

3. Movasaghi, Z.; Rehman, S.; Rehman, I. U., Raman Spectroscopy of Biological Tissues. *Appl. Spectrosc. Rev.* **2007,** *42* (5), 493-541.

4. Szekeres, G. P.; Kneipp, J., Different binding sites of serum albumins in the protein corona of gold nanoparticles. *Analyst* **2018,** *143* (24), 6061-6068.

5. Szekeres, G. P.; Kneipp, J., SERS Probing of Proteins in Gold Nanoparticle Agglomerates. *Front. Chem.* **2019,** *7*, 30.

6. Hornemann, A.; Drescher, D.; Flemig, S.; Kneipp, J., Intracellular SERS hybrid probes using BSA-reporter conjugates. *Anal. Bioanal. Chem.* **2013,** *405* (19), 6209-6222.

7. Lin, V. J.; Koenig, J. L., Raman studies of bovine serum albumin. *Biopolymers* **1976,** *15* (1), 203-18.

8. Drescher, D.; Buchner, T.; McNaughton, D.; Kneipp, J., SERS reveals the specific interaction of silver and gold nanoparticles with hemoglobin and red blood cell components. *Phys. Chem. Chem. Phys.* **2013,** *15* (15), 5364-73.

9. Madzharova, F.; Heiner, Z.; Kneipp, J., Surface Enhanced Hyper-Raman Scattering of the Amino Acids Tryptophan, Histidine, Phenylalanine, and Tyrosine. *J. Phys. Chem. C* **2017,** *121* (2), 1235-1242.